Generality-Oriented Optimization of Enantioselective Aminoxyl Radical Catalysis

Jonas Rein[1†], Soren D. Rozema[2†], Olivia C. Langner[2‡], Samson B. Zacate[1‡], Melissa A. Hardy[3], Juno C. Siu[1], Brandon Q. Mercado[2], Matthew S. Sigman[3]*, Scott J. Miller[2]*, Song Lin[1]*

[1]Department of Chemistry and Chemical Biology, Cornell University; Ithaca, NY 14853, USA.

[2]Department of Chemistry, Yale University; 225 Prospect Street, New Haven, CT 06520, USA.

[3]Department of Chemistry, University of Utah; 315 South 1400 East, Salt Lake City, UT 84112, USA.

[†]These authors contributed equally to this work and are listed in an alphabetical order.

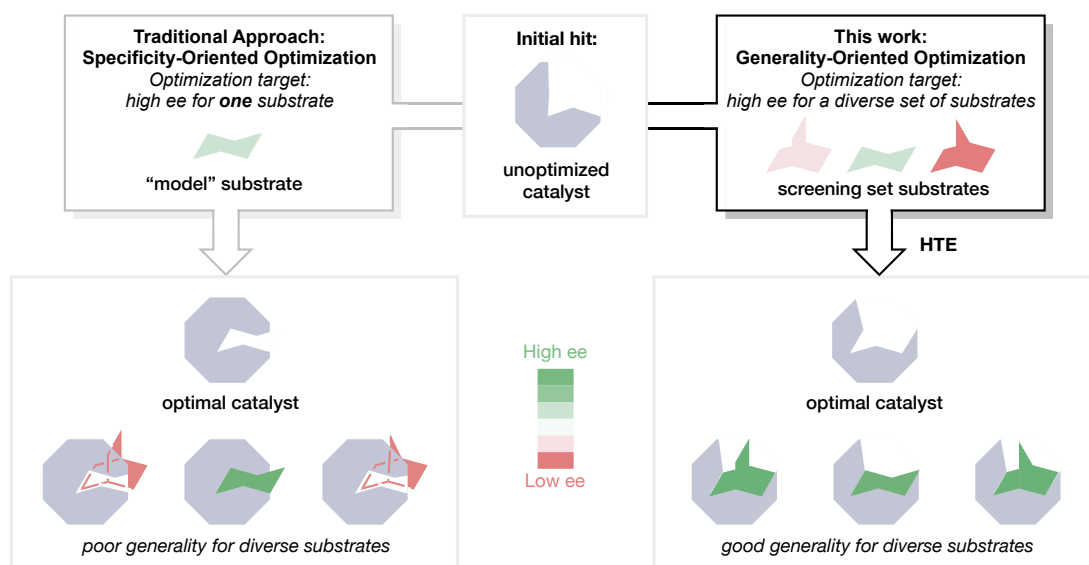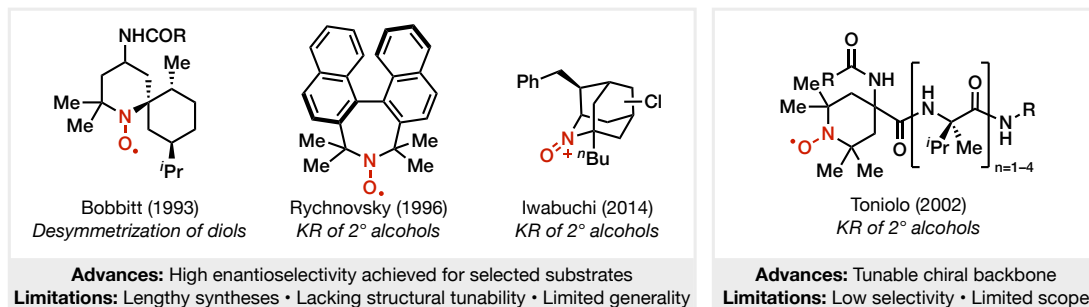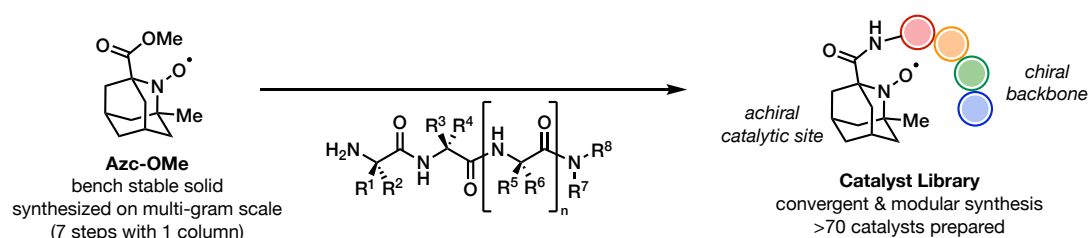[‡]These authors contributed equally to this work and are listed in an alphabetical order.

*Correspondence to: songlin@cornell.edu, scott.miller@yale.edu, matt.sigman@utah.edu

Abstract

Catalytic enantioselective methods that are general over a broad range of substrates facilitate application in synthetic discovery and development settings; however, truly general catalysts for asymmetric synthesis are rare. Herein, we report a strategy for the oxidative desymmetrization of *meso*-1,4 diols predicated on a non-traditional optimization protocol utilizing a panel of screening substrates rather than a singular model substrate. Critical to this approach was rational modulation of a peptide sequence incorporating a novel, aminoxyl-based catalytic residue. A general catalyst emerged, providing high selectivity in delivery of enantioenriched lactones across a broad range of diols.

Main Text

Substrate generality is a longstanding aim in the field of enantioselective catalysis.[1–3] Even so, specificity-oriented optimization has been broadly adopted in the field of small-molecule enantioselective catalysis, resulting in many catalysts that are tailored for one "model" substrate, but often exhibit diminished selectivity upon surveying a diverse substrate scope (Fig. 1A).[4] To address the limited transferability frequently encountered in asymmetric catalysis, we envisioned an optimization strategy with generality as the primary target in catalyst development. This strategy requires parallel screening of a large, diverse catalyst library against a judiciously selected panel of model substrates that represent the chemical space of the target substrate class, rather than a singular substrate.[5] Such an approach is reminiscent of the "one-pot-multi-substrate" method to increase screening throughput.[6–9] However, this pooled-substrate method introduces challenges in chemical compatibility and product analysis, and thus has seen limited implementation in catalyst development. Our interest focused on advancing the notion of generality in the context of previously elusive transformations using a new catalytic platform. Toward this objective, we envisioned that small synthetic, catalytic peptides would be well-suited for such a study, given the modularity of their constituent amino acids and synthetic accessibility, which provides a strong foundation for a generality-driven optimization campaign.[10] Peptide optimization can also bear a resemblance to the venerable directed evolution of enzymes though survey of nth-dimensional catalyst space.[11,12] The current study combines the vast amount of catalyst space surveyed with an expansive substrate space, yielding information rich data that can be utilized for subsequent catalyst optimization. We investigated this strategy in an underexplored area in asymmetric synthesis — enantioselective aminoxyl radical catalysis.[13]

(A) Optimization paradigms in asymmetric catalysis: traditional vs generality-oriented strategies

(B) Precedents for chiral aminoxyl catalysts

Bobbitt (1993)
Desymmetrization of diols

Rychnovsky (1996)
KR of 2° alcohols

Iwabuchi (2014)
KR of 2° alcohols

Toniolo (2002)
KR of 2° alcohols

Advances: High enantioselectivity achieved for selected substrates
Limitations: Lengthy syntheses · Lacking structural tunability · Limited generality

Advances: Tunable chiral backbone
Limitations: Low selectivity · Limited scope

(C) This work: A modular, small-peptide-based platform for aminoxyl asymmetric catalysis

Azc-OMe
bench stable solid
synthesized on multi-gram scale
(7 steps with 1 column)

Catalyst Library
convergent & modular synthesis
>70 catalysts prepared

Figure 1. Conceptual outline of a generality-oriented optimization strategy toward the development of enantioselective catalysis with peptidyl aminoxyl radicals. **(A)** Optimization paradigms in asymmetric catalysis: traditional vs generality-oriented strategies. **(B)** Precedence for chiral aminoxyl and oxoammonium catalysts.[23] **(C)** This work: A modular, small-peptide-based platform for aminoxyl asymmetric catalysis.
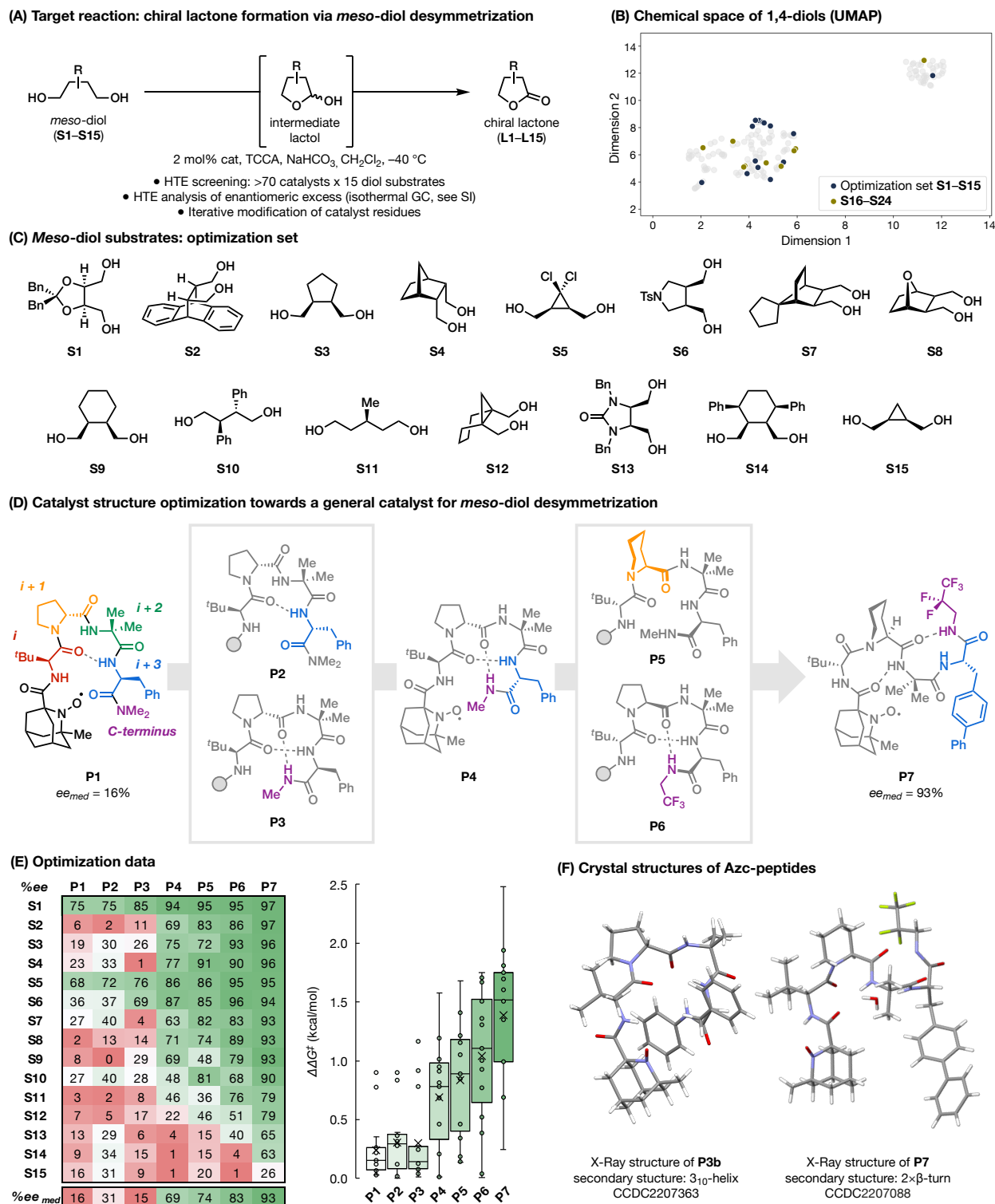
Aminoxyl radicals are a class of persistent open-shell molecules that have found broad applications in organic synthesis.[14] They have been shown as excellent catalysts for the oxidation of various functional groups such as alcohols, amines, and alkenes via intermediate oxoammonium ions.[14–19] In contrast to the vast number of reactions known to be catalyzed by aminoxyl radicals, enantioselective variants remain rare. Foundational work by Bobbitt and recent advances by Iwabuchi provided salient precedents in asymmetric alcohol oxidation (Fig. 1B).[20–22] Nevertheless, these catalysts require lengthy synthetic preparation and lack the structural modularity needed for generality-oriented optimization. Toniolo and co-workers demonstrated that

oxoammonium ions are compatible within peptidic frameworks and observed enantioselectivity in the kinetic resolution of a singular substrate with modest selectivities (k_{rel} < 3).[13] In light of these precedents, we hypothesized that incorporation of an achiral aminoxyl moiety into diverse peptide-based scaffolds could provide a catalyst platform that would enable exploration of generality within the reaction space accessible to aminoxyl catalysis. Accordingly, we designed and synthesized an aminoxyl monomer (**Azc-OMe**, Fig. 1C) that could be readily incorporated into peptides enabling the preparation of a library of >70 chiral catalysts. Herein, we report the development of the highly enantioselective desymmetrization of *meso*-diols using aminoxyl-based oligopeptides, for which a generality-oriented optimization campaign led to a unique and versatile catalyst that delivers high selectivity for structurally diverse chiral lactones.

We initiated our study with the desymmetrization of *meso*-diols (Fig. 2A). In the presence of a chiral catalyst, diol substrate **S** underwent selective oxidation at one of the enantiotopic hydroxyl groups, with the other hydroxyl group cyclized onto the incipient aldehyde to furnish an intermediate lactol. Subsequent second oxidation delivered chiral lactone **L**, a class of compounds displaying biological activity and utility as building blocks in organic and materials synthesis (*vide infra*). We initially utilized a traditional approach by screening a collection of aminoxyl-embedded peptide catalysts in the oxidation of 1,4-diol **S1**, employing trichloroisocyanuric acid (TCCA) as terminal oxidant and sodium bicarbonate as base.[21,22] This effort yielded peptide **P1** that provided lactone **L1** with substantial enantioselectivity (*ee* = 75%). However, **P1** showed diminished selectivity when tested against an array of additional 1,4-diols displaying a variety of steric and electronic profiles, giving a median *ee* of only 16% (Fig. 2E, column **P1**). This result underscores the challenge of identifying highly selective catalysts that tolerate a broad scope when focusing on a singular substrate during catalyst optimization.

Aiming for a more general method, we assessed a diverse library of peptide scaffolds with high-throughput experimentation (HTE) using 24-well plate parallel screening and GC analysis. Employing this workflow, the data obtained with a given catalyst is discussed below in terms of the *median ee* (*ee_med*), which served as the primary optimization target; excellent conversion for each substrate allowed us to remain agnostic to yield throughout optimization. Substrate selection was guided by mapping the chemical space of commercially available 1,4-*meso*-diols to ensure diversity of the screening set (Fig. 2B). This analysis revealed two clusters of diols, with the larger cluster representing di-substituted *meso*-diols and the smaller cluster consisting of a unique group of 2,2,3,3-tetrasubstitued 1,4-diols. From this collection of compounds, 15 structurally diverse substrates with a variety of functionality were included in the model set that effectively sampled the chemical space, consisting of eight monocyclic (**S1**, **S3**, **S5**, **S6**, **S9**, **S13**–**15**) and five polycyclic (**S2**, **S4**, **S7**, **S8**, **S12**) substrates with various ring sizes, as well as one acyclic diol (**S10**) (Fig. 2C). Additionally, a 1,5-diol (**S11**) was included to further increase diversity in the optimization set.

With this set of model substrates, catalysts were then evaluated as a function of their constituent residues (Fig. 2D). Beginning with **P1** (*ee_med* = 16%), two single point changes exhibited increases in *ee_med*: inversion of stereochemistry at *i+3* (**P2**) provided *ee_med* of 31% and replacement of the *NMe_2* group at the *C*-terminus with *NHMe* (**P3**) provided an *ee_med* of 15% but displayed considerable improvement for three substrates (**S1**, **S6**, **S9**). Auspiciously, **P3b**, an analog of **P3**, was crystalline; allowing for the secondary structure of this catalyst to be determined by X-ray crystallography (Fig. 2F) and confirmed by ROESY NMR to adopt a 3_{10}-helical motif in solution.[24] Notably, the confluence of changes producing **P2** and **P3** from **P1** was found to be beneficial; **P4**, possessing both the optimized relative stereochemistry of **P2** and the *NHMe C*-terminus of **P3**, provided a significant enhancement in selectivity with an *ee_med* of 69% (**P4**). Further modifications to **P4** showed that two additional point changes furnished substantial enhancement in *ee_med*: replacement of the 5-membered proline (Pro) with the 6-membered homologue pipecolic acid (Pip) at *i+1* (**P5**) led to an increase of *ee_med* to 74%; concurrently, the inclusion of an *NHCH_2CF_3* substituent at the C-terminal position resulted in peptide **P6** that greatly

(A) Target reaction: chiral lactone formation via *meso*-diol desymmetrization

meso-diol
(**S1–S15**)

intermediate
lactol

chiral lactone
(**L1–L15**)

2 mol% cat, TCCA, NaHCO$_3$, CH$_2$Cl$_2$, –40 °C
- HTE screening: >70 catalysts x 15 diol substrates
- HTE analysis of enantiomeric excess (isothermal GC, see SI)
- Iterative modification of catalyst residues

(B) Chemical space of 1,4-diols (UMAP)

(C) *Meso*-diol substrates: optimization set

(D) Catalyst structure optimization towards a general catalyst for *meso*-diol desymmetrization

P1
ee_{med} = 16%

P2

P3

P4

P5

P6

P7
ee_{med} = 93%

(E) Optimization data

%ee	P1	P2	P3	P4	P5	P6	P7
S1	75	75	85	94	95	95	97
S2	6	2	11	69	83	86	97
S3	19	30	26	75	72	93	96
S4	23	33	1	77	91	90	96
S5	68	72	76	86	86	95	95
S6	36	37	69	87	85	96	94
S7	27	40	4	63	82	83	93
S8	2	13	14	71	74	89	93
S9	8	0	29	69	48	79	93
S10	27	40	28	48	81	68	90
S11	3	2	8	46	36	76	79
S12	7	5	17	22	46	51	79
S13	13	29	6	4	15	40	65
S14	9	34	15	1	15	4	63
S15	16	31	9	1	20	1	26
%ee $_{med}$	16	31	15	69	74	83	93

$\Delta\Delta G^{\ddagger}$ (kcal/mol)

P1 P2 P3 P4 P5 P6 P7

(F) Crystal structures of Azc-peptides

X-Ray structure of **P3b**
secondary structure: 3$_{10}$-helix
CCDC2207363

X-Ray structure of **P7**
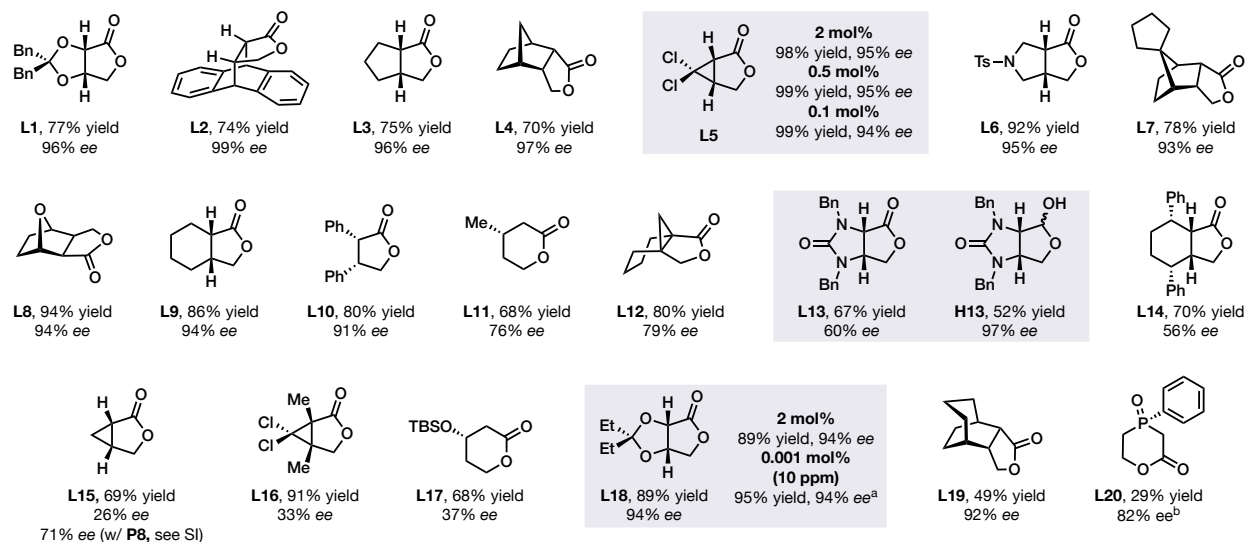secondary structure: 2×β-turn
CCDC2207088

Figure 2. Generality-oriented optimization through combinatorial screening of catalysts with a substrate library and iterative modification of catalyst structure. **(A)** Chiral lactone formation via *meso*-diol desymmetrization. **(B)** Chemical space of *meso*-1,4-diols defined using Mordred descriptors and a uniform manifold approximation and projection (UMAP) with molecular fingerprints of commercial *meso*-1,4-diols from a Reaxys® search. **(C)** *Meso*-diol substrates: optimization set. **(D)** catalyst structure optimization. **(E)** optimization data. **(F)** Crystal structures of peptides **P3b** and **P7**.

outperforms catalysts with other *C*-termini, presenting an ee_{med} of 83%. Catalyst **P7**, combining the Pip residue found in **P5** with an elongated perfluorinated *C*-terminus ($NHCH_2C_2F_5$) and a change to biphenylalanine (Bip) at *i+3* gave a further boost of ee_{med} to 93% with 10 of 15 substrates showing >90% *ee*, and an additional four substrates displaying *ee* >60%. X-ray analysis and ROESY NMR were also performed on **P7**, revealing that both the aminoxyl radical and the active oxoammonium forms of the catalyst share secondary structural features. Notably, the solid-state structure of **P7** shows a departure from the 3_{10}-helix observed in **P3b**, displaying instead two successive β-turns (Fig. 2F).[25] Provided the success of the parallel optimization campaign, particular challenges for certain substrates persisted. For example, throughout the optimization, one diol (**S15**) was recalcitrant towards significant selectivity enhancement, delivering only 26% *ee* with **P7**. Parenthetically, a structurally distinct catalyst **P8** was identified that provided 71% *ee* for the corresponding lactone **L15**.
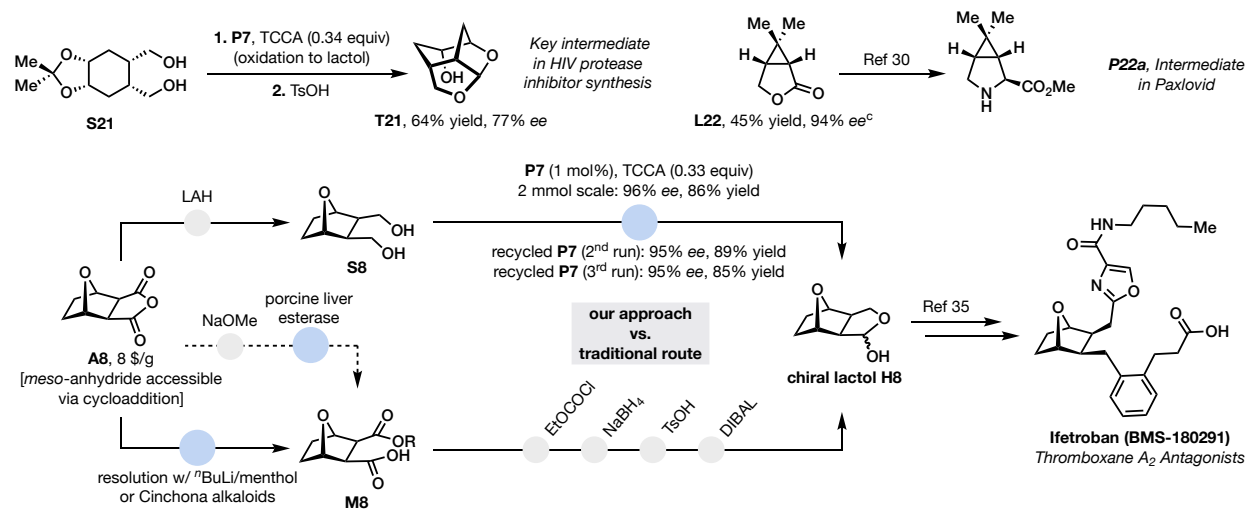
We then probed the scope and limitations associated with catalyst **P7** through desymmetrization on a 0.2-mmol scale (Fig. 3A). Chiral lactones are valuable and versatile building blocks in organic and polymer synthesis. While highly selective methods are available for synthesizing specific types of enantioenriched lactones, a general approach that is agnostic of substrate structure and substitution remains elusive and desirable. We found that ketal protected erythronic acid γ-lactones **L1** and **L18** were formed in good yields and excellent enantioenrichment. Polycyclic diols were efficiently desymmetrized (**L2**, **L4**, **L7**, **L8**, **L19**), providing valuable precursors for pharmaceuticals and chiral ligands.[26–28] Cyclopentane lactone **L3** and fungistatic cyclohexane lactone **L9**[29] were formed with 96% *ee* and 94% *ee*, respectively. Further evaluation of cyclopropyl diols revealed a requirement for substitution on the ring for high selectivity. While unsubstituted **L15** was accessed in only 26% *ee*, dichloro- and dimethylcyclopropane lactones **L5** and **L22** were produced with excellent enantioselectivity, the latter of which is a key intermediate in the preparation of numerous natural and unnatural products including COVID drug Nirmatrelvir (Paxlovid) (Fig. 3B).[30,31] Pyrrolidine-bearing **S6** was desymmetrized with excellent yield (92%) and selectivity (95% *ee*). Linear 1,4-diols were also efficient substrates in this reaction, as lactone **L10** was obtained in 80% yield and 91% *ee*. In a dramatic test of our approach, the desymmetrization of a prochiral linear 1,5-diol bearing a mere methyl group at the central carbon was transformed to δ-lactone **L11** with 76% *ee*, providing access to a monomer for a biodegradable isotactic polymer.[32] Notably, the catalyst is also competent in desymmetrizing a prochiral-at-phosphorous 1,5-diol, affording lactone **L20** in 82% *ee*. An additional 1,5-diol exhibited lower selectivity, with **L17** being enriched to only 37% *ee*. Tetrasubstituted diols are also tolerated with bicyclic substrate **S12** yielding a [4.3.1] propellane in 80% yield and 79% *ee*; tetrasubstituted lactone **L16**, however, was obtained in only 33% *ee*. Diphenylcyclohexyl diol **S14**, which throughout optimization gave poor selectivities, was desymmetrized up to 56% *ee*. Urea **L13**, a valuable chiral intermediate in the chemical synthesis of biotin, was accessed in 60% *ee*.[33] Markedly, a kinetic resolution of intermediate **H13** was observed, which preferentially oxidized its minor enantiomer to **L13** and allowed for the isolation of **H13** in 52% yield and 97% *ee* when the reaction was stopped at an early stage.

Catalyst **P7** exhibits high chemoselectivity for oxidation of diols over lactols (see Fig. 4b), which enabled direct access to these valuable synthons by reducing the oxidant stoichiometry. We showcased this method in the concise formal synthesis of two pharmaceutical candidates, improving upon previous routes in step count. Thus, tricyclic **T21**, a key intermediate in the synthesis of an HIV protease inhibitor,[34] was obtained through oxidation of acetonide **S21** followed by one-pot acid-mediated transacetalization in 64% overall yield with 77% *ee* (Fig. 3B). In a second example, lactol **H8**, an intermediate in the synthesis of thromboxane receptor antagonist *Ifetoban*,[35] currently in clinical trials, was obtained on 2 mmol scale in 96% *ee* and 86% yield via an expedient two-step process from commercial *meso*-acid anhydride **A8**.[36] In contract, traditional syntheses required enantioselective methanolysis of **A8** to form mono-ester **M8** followed by a sequence of redundant functional group interconversions and redox manipulations.[37,38]
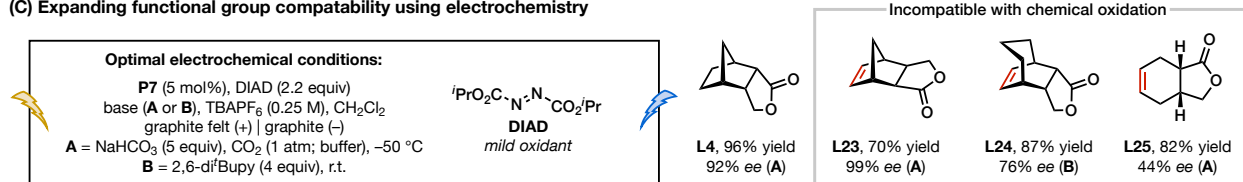
(A) Substrate scope using catalyst P7

L1, 77% yield 96% ee

L2, 74% yield 99% ee

L3, 75% yield 96% ee

L4, 70% yield 97% ee

L5 — 2 mol% 98% yield, 95% ee / 0.5 mol% 99% yield, 95% ee / 0.1 mol% 99% yield, 94% ee

L6, 92% yield 95% ee

L7, 78% yield 93% ee

L8, 94% yield 94% ee

L9, 86% yield 94% ee

L10, 80% yield 91% ee

L11, 68% yield 76% ee

L12, 80% yield 79% ee

L13, 67% yield 60% ee

H13, 52% yield 97% ee

L14, 70% yield 56% ee

L15, 69% yield 26% ee 71% ee (w/ **P8,** see SI)

L16, 91% yield 33% ee

L17, 68% yield 37% ee

L18, 89% yield 94% ee — 2 mol% 89% yield, 94% ee / 0.001 mol% (10 ppm) 95% yield, 94% ee[a]

L19, 49% yield 92% ee

L20, 29% yield 82% ee[b]

(B) Utility in the synthesis of drug molecules

S21

1. **P7**, TCCA (0.34 equiv) (oxidation to lactol)
2. TsOH

T21, 64% yield, 77% ee

Key intermediate in HIV protease inhibitor synthesis

L22, 45% yield, 94% ee[c]

Ref 30

P22a, Intermediate in Paxlovid

LAH

S8

P7 (1 mol%), TCCA (0.33 equiv) 2 mmol scale: 96% ee, 86% yield

recycled **P7** (2nd run): 95% ee, 89% yield
recycled **P7** (3rd run): 95% ee, 85% yield

A8, 8 $/g
[*meso*-anhydride accessible via cycloaddition]

NaOMe / porcine liver esterase

resolution w/ *n*BuLi/menthol or Cinchona alkaloids

M8

our approach vs. traditional route

EtOCOCl / NaBH4 / TsOH / DIBAL

chiral lactol H8

Ref 35

Ifetroban (BMS-180291)
Thromboxane A2 Antagonists

(C) Expanding functional group compatability using electrochemistry

Optimal electrochemical conditions:
P7 (5 mol%), DIAD (2.2 equiv)
base (**A** or **B**), TBAPF6 (0.25 M), CH2Cl2
graphite felt (+) | graphite (–)
A = NaHCO3 (5 equiv), CO2 (1 atm; buffer), –50 °C
B = 2,6-di*t*Bupy (4 equiv), r.t.

*i*PrO2C–N=N–CO2*i*Pr
DIAD
mild oxidant

L4, 96% yield 92% ee (**A**)

Incompatible with chemical oxidation

L23, 70% yield 99% ee (**A**)

L24, 87% yield 76% ee (**B**)

L25, 82% yield 44% ee (**A**)

Figure 3. Substrate scope. Absolute stereochemistry was assigned by analogy to **L1**, **L4**, and **L6**. [a]0.001 mol% **P7**, 96 h, –50 °C, then 2 mol% ACT, 0.3 equiv TCCA, r.t., 6 h. [b]Isolated as the methyl ester after SiO2 catalyzed methanolysis. [c]10 mol% **P7**. **(a)** Substrate scope using **P7**. **(b)** Utility of products in drug molecules. **(c)** Expansion of functional group compatibility using electrochemistry.
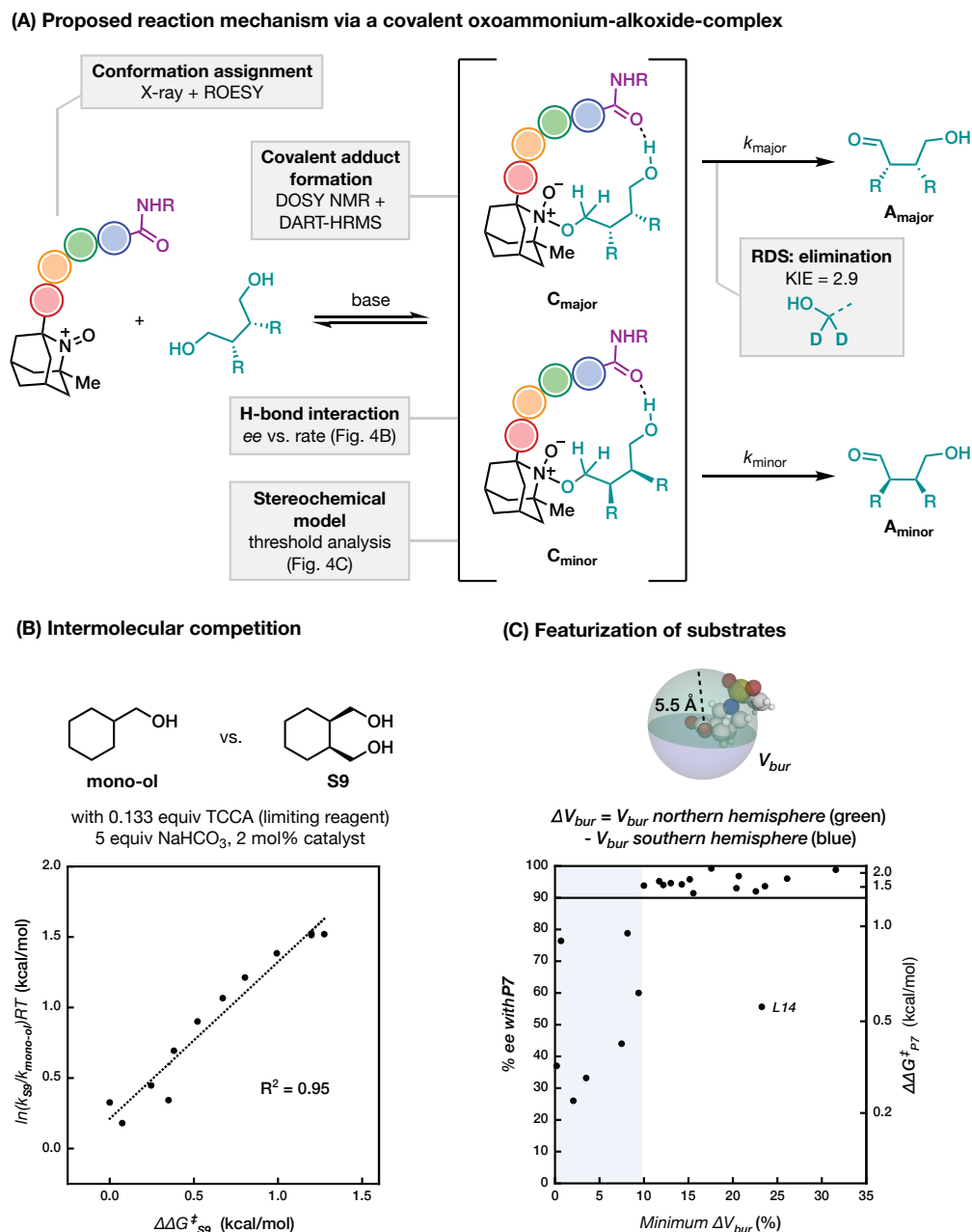
While the optimal conditions using TCCA tolerated substrates with diverse steric and electronic profiles, the scope was limited to compounds that were compatible in the presence of a strong chemical oxidant. Indeed, substrates containing alkenes were chlorinated, resulting in diminished yields (0–25%). Such products are nonetheless important synthetic intermediates; for example, unsaturated **L23** was leveraged in the preparation of a thromboxane-A2 antagonist.[39,40]

To address this issue, an electrochemical protocol was developed. The key was to identify a sacrificial oxidant that would not decompose sensitive substrates but would allow for the desired electrochemical reaction to take place in the presence of an electric driving force.[41] In traditional anodic oxidation reactions, protic acids or alkyl halides[42] are used as sacrificial oxidants, but these species proved incompatible in our reaction system likely due to the liberation of Lewis basic anions during their cathodic reduction that led to detrimental catalyst binding. Rapid screening using parallel reactor HTe⁻Chem led to the identification of two classes of oxidants that provided high yields and enantioselectivities: dialkyl azodicarboxylates and disubstituted peroxides. We found that diisopropyl azodicarboxylate (DIAD) proved to be optimal, providing products **L23–25** in good yields and high enantioselectivity, while itself was reduced to innocuous diisopropyl hydrazine-1,2-dicarboxylate (Fig. 3C). In this case, either an organic base 2,6-di-*tert*-butylpyridine or an inorganic buffer consisting of $NaHCO_3$ and CO_2 were used.

To establish the upper limit of catalytic turnover, we surveyed decreased catalyst loadings using diethyl ketal **S18** and found that even 0.001 mol% catalyst (10 ppm; 2,000-fold decrease from standard 2 mmol% conditions) promoted the reaction without any loss in yield or enantioselectivity. Thus, **P7** achieved ~1.2×10^5 turnovers, to our knowledge the highest number recorded for an oligopeptide organocatalyst.[43] The catalyst could also be recycled and reused multiple times as shown in the synthesis of **H8**, further demonstrating the potential practicality of the reported protocol.

Finally, we conducted studies to gain understanding of the mechanistic underpinnings of the observed substrate generality and high enantioselectivity (Fig. 4A). The composition of the resting state of the catalyst was interrogated using in situ diffusion-ordered spectroscopy (DOSY) NMR experiments and direct analysis in real time (DART) high-resolution mass spectrometry, showing the formation of oxoammonium-alkoxide complexes (**C**) between the catalyst and the diol substrate. Further kinetic isotope effect studies support that the rate-determining step of the reaction is a Cope-elimination from the resting state adduct to provide the desymmetrized aldehyde intermediates (**A**).[14] Subsequently, a suite of kinetic experiments was performed to probe additional catalyst-substrate interactions. Intermolecular competition studies between diol **S9** and mono-ol, cyclohexylmethanol, established excellent correlation ($R^2 = 0.95$) between the enantioenrichment of **L9** ($\Delta\Delta G^\ddagger$) and the relative reaction rate of **S9** vs mono-ol ($\ln(k_{diol}/k_{mono\text{-}ol})RT$) (Fig. 2B). More enantioselective catalysts showed a higher degree of selectivity towards diol over mono-ol oxidation with up to a 26-fold rate difference. These findings depict a structure wherein the spectator alcohol participates in hydrogen bonding with a functional group on the peptide backbone (Fig. 4A), in addition to the covalent association of the reacting alcohol and the oxoammonium catalytic unit. Consistent with this, substrate features can be used to quantitatively classify when a substrate should perform well in this reaction. Using a threshold value of 90% *ee*, substrates can be classified based on the difference between the buried volumes ($V_{bur}\%$) of each face of the lactone motif (Fig. 4C), revealing that substrates with a minimum $\Delta V_{bur}\%$ of greater than 10% provide excellent enantioselectivity.

Taken together, positing that the diol motif provides robust two-point binding with the catalyst, the substituents on the substrate backbone imparts steric differentiation between the opposing diastereometric transition states, thereby providing a basis for the observed high enantioselectivity. This mechanism of stereoinduction is effective for a wide range of diols with distinct structures and functional groups, resulting in the observed substrate generality.

(A) Proposed reaction mechanism via a covalent oxoammonium-alkoxide-complex

(B) Intermolecular competition

mono-ol vs. **S9**

with 0.133 equiv TCCA (limiting reagent)
5 equiv NaHCO₃, 2 mol% catalyst

$R^2 = 0.95$

(C) Featurization of substrates

5.5 Å

V_{bur}

$\Delta V_{bur} = V_{bur}$ *northern hemisphere* (green)
- V_{bur} *southern hemisphere* (blue)

Figure 4. Mechanistic analysis. **(a)** mechanistic analysis. **(b)** Intermolecular competition studies. **(c)** Featurization of products.

References:

1.   Yoon, T. P.; Jacobsen, E. N. Privileged Chiral Catalysts. *Science* **2003**, *299*, 1691-1693.
2.   Jacobsen, E. N.; Pfaltz, A.; Yamamoto, H., *Comprehensive Asymmetric Catalysis*. Springer: **1999**; Vol. I to III.
3.   Strassfeld, D. A.; Algera, R. F.; Wickens, Z. K.; Jacobsen, E. N. A Case Study in Catalyst Generality: Simultaneous, Highly-Enantioselective Brønsted- and Lewis-Acid Mechanisms in Hydrogen-Bond-Donor Catalyzed Oxetane Openings. *J. Am. Chem. Soc.* **2021**, *143*, 9585-9594.
4.   Wagen, C. C.; McMinn, S. E.; Kwan, E. E.; Jacobsen, E. N. Screening for Generality in Asymmetric Catalysis. *Nature* **2022**, *610*, 680-686.
5.   During preparation of this manuscript, Jacobsen and co-workers reported a pooled-product method for enantioselectivity analysis, which enabled high-throughput evaluation of the generality of known catalysts in the context of an asymmetric Pictet-Spengler reaction. See ref. 4.
6.   X Gao, X.; Kagan, H. B. One-pot multi-substrate screening in asymmetric catalysis. *Chirality* **1998**, *10*, 120-124.
7.   Satyanarayana, T.; Kagan, H. B. The Multi-Substrate Screening of Asymmetric Catalysts. *Adv. Synth. Catal.* **2005**, *347*, 737-748.
8.   Kim, H.; Gerosa, G.; Aronow, J.; Kasaplar, P.; Ouyang, J.; Lingnau, J. B.; Guerry, P.; Farès, C.; List, B. A multi-substrate screening approach for the identification of a broadly applicable Diels–Alder catalyst. *Nat. Commun.* **2019**, *10*, 770.
9.   Burgess, K.; Lim, H.-J.; Porte, A. M.; Sulikowski, G. A. New Catalysts and Conditions for a C-H Insertion Reaction Identified by High Throughput Catalyst Screening. *Angew. Chem. Int. Ed.* **1996**, *35*, 220-222.
10.   Metrano, A. J.; Chinn, A. J.; Shugrue, C. R.; Stone, E. A.; Kim, B.; Miller, S. J. Asymmetric Catalysis Mediated by Synthetic Peptides, Version 2.0: Expansion of Scope and Mechanisms. *Chem. Rev.* **2020**, *120*, 11479-11615.
11.   Wang, Y; Cao, M; Yu, T.;Lane, S. T.; Zhao, H. Directed Evolution: Methodologies and Applications. *Chem. Rev.* **2021**, *121*, 12384-12444.
12.   Lichtor, P. A.; Miller S. J. Combinatorial evolution of site- and enantioselective catalysts for polyene epoxidation. *Nat. Chem.* **2012**, *4*, 990-995.
13.   Formaggio, F.; Bonchio, M.; Crisma, M.; Peggion, C.; Mezzato, S.; Polese, A.; Barazza, A.; Antonello, S.; Maran, F.; Broxterman, Q. B.; Kaptein, B.; Kamphuis, J.; Vitale, R. M.; Saviano, M.; Benedetti, E.; Toniolo, C. Nitroxyl Peptides as Catalysts of Enantioselective Oxidations. *Chem. Eur. J.* **2002**, *8*, 84-93.
14.   Nutting, J. E.; Rafiee, M.; Stahl, S. S. Tetramethylpiperidine N-Oxyl (TEMPO), Phthalimide N-Oxyl (PINO), and Related N-Oxyl Species: Electrochemical Properties and Their Use in Electrocatalytic Reactions. *Chem. Rev.* **2018**, *118*, 4834-4885.
15.   Siu, J. C.; Parry, J. B.; Lin, S. Aminoxyl-Catalyzed Electrochemical Diazidation of Alkenes Mediated by a Metastable Charge-Transfer Complex. *J. Am. Chem. Soc.* **2019**, *141*, 2825-2831.

16. Bobbitt, J. M.; Brückner, C.; Merbouh, N., Oxoammonium- and Nitroxide-Catalyzed Oxidations of Alcohols. In *Organic Reactions*; Wiley, **2010**; pp 103-424.

17. Nagasawa, S.; Sasano, Y.; Iwabuchi, Y. The Utility of Oxoammonium Species in Organic Synthesis: Beyond Alcohol Oxidation. *Heterocycles* **2022**, *105*, 61-114.

18. Semmelhack, M. F.; Schmid, C. R. Nitroxyl-mediated electro-oxidation of amines to nitriles and carbonyl compounds. *J. Am. Chem. Soc.* **1983**, *105*, 6732-6734.

19. Wang, F.; Rafiee, M.; Stahl, S. S. Electrochemical Functional-Group-Tolerant Shono-type Oxidation of Cyclic Carbamates Enabled by Aminoxyl Mediators. *Angew. Chem. Int. Ed.* **2018**, *57*, 6686-6690.

20. Ma, Z.; Huang, Q.; Bobbitt, J. M. Oxoammonium salts. 5. A new synthesis of hindered piperidines leading to unsymmetrical TEMPO-type nitroxides. Synthesis and enantioselective oxidations with chiral nitroxides and chiral oxoammonium salts. *J. Org. Chem.* **1993**, *58*, 4837-4843.

21. Murakami, K.; Sasano, Y.; Tomizawa, M.; Shibuya, M.; Kwon, E.; Iwabuchi, Y. Highly Enantioselective Organocatalytic Oxidative Kinetic Resolution of Secondary Alcohols Using Chiral Alkoxyamines as Precatalysts: Catalyst Structure, Active Species, and Substrate Scope. *J. Am. Chem. Soc.* **2014**, *136*, 17591-17600.

22. Tomizawa, M.; Shibuya, M.; Iwabuchi, Y. Highly Enantioselective Organocatalytic Oxidative Kinetic Resolution of Secondary Alcohols Using Chirally Modified AZADOs. *Org. Lett.* **2009**, *11*, 1829-1831.

23. Rychnovsky, S. D.; McLernon, T. L.; Rajapakse, H. Enantioselective Oxidation of Secondary Alcohols Using a Chiral Nitroxyl (N-Oxoammonium salt) Catalyst. *J. Org. Chem.* **1996**, *61*, 1194-1195.

24. Hutchinson, E. G.; Thornton, J. M. A revised set of potentials for β-turn formation in proteins. *Protein Sci.* **1994**, *3*, 2207-2216.

25. Metrano, A. J.; Abascal, N. C.; Mercado, B. Q.; Paulson, E. K.; Hurtley, A. E.; Miller, S. J. Diversity of Secondary Structure in Catalytic Peptides with β-Turn-Biased Sequences. *J. Am. Chem. Soc.* **2017**, *139*, 492-516.

26. Trost, B. M.; Vidal, B.; Thommen, M. Novel Chiral Bidentate η5-Cyclopentadienylphosphine Ligands: Their Asymmetric Induction at the Ruthenium(II) Center and Application in Catalysis. *Chem. Eur. J.* **1999**, *5*, 1055-1069.

27. Kametani, T.; Suzuki, T.; Kamada, S.; Unno, K. Synthesis of the prostaglandin H2 analogue DL-9,11-ethano-9,11-dideoxaprostaglandin H2. *J. Chem. Soc., Perkin Trans. I* **1981**, 3101-3105.

28. Hagishita, S.; Seno, K. Thromboxane A_2 Receptor Antagonists. I. : Synthesis and Pharmacological Activity of 7-Oxabicyclo-[2.2.1]heptane Derivatives with the Benzenesulfonylamino Group. *Chem. Pharm. Bull.* **1989**, *37*, 327-335.

29. Olejniczak, T.; Boratyński, F.; Białońska, A. Fungistatic Activity of Bicyclo[4.3.0]-γ-lactones. *J. Agric. Food Chem.* **2011**, *59*, 6071-6081.

30. Thierry, B.; Patrice, D. Nouveau procede de synthese du (1r,2s,5s)-6,6-dimethyl-3-azabicyclo[3.1.0]hexane-2-carboxylate de methyle ou de l'un de ses sels. France FR2972453 **2012**.

31. Löffler, L. E.; Wirtz, C.; Fürstner, A. Collective Total Synthesis of Casbane Diterpenes: One Strategy, Multiple Targets. *Angew. Chem. Int. Ed.* **2021**, *60*, 5316-5322.

32. Zhang, C.; Schneiderman, D. K.; Cai, T.; Tai, Y.-S.; Fox, K.; Zhang, K. Optically Active β-Methyl-δ-Valerolactone: Biosynthesis and Polymerization. *ACS Sustain. Chem. Eng.* **2016**, *4*, 4396-4402.

33. Seki, M.; Takahashi, Y. Practical Synthesis of (+)-Biotin Key Intermediate by Calcium Borohydride Reduction and Temperature-Dependent Purity Upgrade during Crystallization. *Org. Process Res. Dev.* **2021**, *25*, 1950-1959.

34. Ghosh, A. K.; Kovela, S.; Osswald, H. L.; Amano, M.; Aoki, M.; Agniswamy, J.; Wang, Y.-F.; Weber, I. T.; Mitsuya, H. Structure-Based Design of Highly Potent HIV-1 Protease Inhibitors Containing New Tricyclic Ring P2-Ligands: Design, Synthesis, Biological, and X-ray Structural Studies. *J. Med. Chem.* **2020**, *63*, 4867-4879.

35. Misra, R. N., Brown, B. R.; Sher, P. M.; Patel, M. M.; Hall, S. E.; Han, W. C.; Barrish, J. C.; Kocy, O.; Harris, D. N.; Goldenberg, H. J.; Michel, I. M.; Schumacher, W. A.; Webb, M. L.; Monshizadegan, H.; Ogletree, M. L. Interphenylene 7-oxabicyclo[2.2.1]heptane oxazoles. Highly potent, selective, and long-acting thromboxane A$_2$ receptor antagonists. *J. Med. Chem.* **1993**, *36*, 1401-1417.

36. Rosenfeld, L.; Grover, G. J.; Stier Jr., C. T. Ifetroban Sodium: An Effective TxA$_2$/PGH$_2$ Receptor Antagonist. *Cardiovasc. Drug Rev.* **2001**, *19*, 97-115.

37. Das, J.; Haslanger, M. F.; Gougoutas, J. Z.; Malley, M. F. Synthesis of Optically Active 7-Oxabicyclo[2.2.1]heptanes and Assignment of Absolute Configuration. *Synthesis* **1987**, *12*, 1100-1103.

38. Chen, Y.; Tian S.-K.; Deng, L. A Highly Enantioselective Catalytic Desymmetrization of Cyclic Anhydrides with Modified Cinchona Alkaloids. *J. Am. Chem. Soc.* **2000**, *122*, 9542-9543.

39. Takano, S.; Inomata, K.; Kurotaki, A.; Ohkawa, T.; Ogasawara, K. Enantiodivergent route to both enantiomers of β-santalene and epi-β-santalene from a single chiral template. *J. Chem. Soc. Chem. Commun.* **1987**, 1720-1722.

40. Lieb, F.; Niewöhner, U.; Wendisch, D. 6-(3-Carbamoylbicyclo[2.2.1]hept-2-yl)hexansäuren, eine neue Klasse von TxA2-Antagonisten. *Liebigs Ann. Chem.* **1987**, *1987*, 607-615.

41. Rein, J.; Annand, J. R.; Wismer, M. K.; Fu, J.; Siu, J. C.; Klapars, A.; Strotman, N. A.; Kalyani, D.; Lehnherr, D.; Lin, S. Unlocking the Potential of High-Throughput Experimentation for Electrochemistry with a Standardized Microscale Reactor. *ACS Cent. Sci.* **2021**, *7*, 1347-1355.

42. Dong, X.; Roeckl, J. L.; Waldvogel, S.R.; Morandi, B. Merging shuttle reactions and paired electrolysis for reversible vicinal dihalogenations. *Science* **2021**, *371*, 507-514.

43. Giacalone, F.; Gruttadauria, M.; Agrigento, P.; Noto, R. Low-loading asymmetric organocatalysis. *Chem. Soc. Rev.* **2012**, *41*, 2406-2447.